

Microfluidic Affinity Profiling reveals a Broad Range of Target Affinities for Anti-SARS-CoV-2 Antibodies in Plasma of Covid Survivors

Matthias M. Schneider^{1,#}, Marc Emmenegger^{2,#}, Catherine K. Xu^{1,#}, Itzel Condado Morales^{2,#}, Priscilla Turelli³, Manuela R. Zimmermann¹, Beat M. Frey⁴, Sebastian Fiedler⁵, Viola Denninger⁵, Georg Meisl¹, Vasilis Kosmoliaptsis^{6,7}, Heike Fiegler⁵, Didier Trono³, Tuomas P. J. Knowles^{1,8*}, and Adriano Aguzzi^{2*}

¹ Centre for Misfolding Diseases, Department of Chemistry, University of Cambridge, Lensfield Road, Cambridge CB2 1EW, United Kingdom

² Institute of Neuropathology, University of Zurich, 8091 Zurich, Switzerland

³ School of Life Sciences, École Polytechnique Fédérale de Lausanne, Lausanne, Switzerland

⁴ Regional Blood Transfusion Service Zurich, Swiss Red Cross, 8952 Schlieren, Switzerland

⁵ Fluidic Analytics, Unit A, The Paddocks Business Centre, Cherry Hinton Rd, Cambridge CB1 8DH, UK

⁶ Department of Surgery, Addenbrooke's Hospital, University of Cambridge, Hills Road, Cambridge CB2 0QQ, United Kingdom

⁷ NIHR Blood and Transplant Research Unit in Organ Donation and Transplantation, University of Cambridge, Hills Road, Cambridge CB2 0QQ, United Kingdom

⁸ Cavendish Laboratory, Department of Physics, University of Cambridge, JJ Thomson Ave, Cambridge CB3 0HE, United Kingdom

equal contribution

*to whom correspondence should be addressed: adriano.aguzzi@usz.ch or tpjk2@cam.ac.uk

Supplementary Information

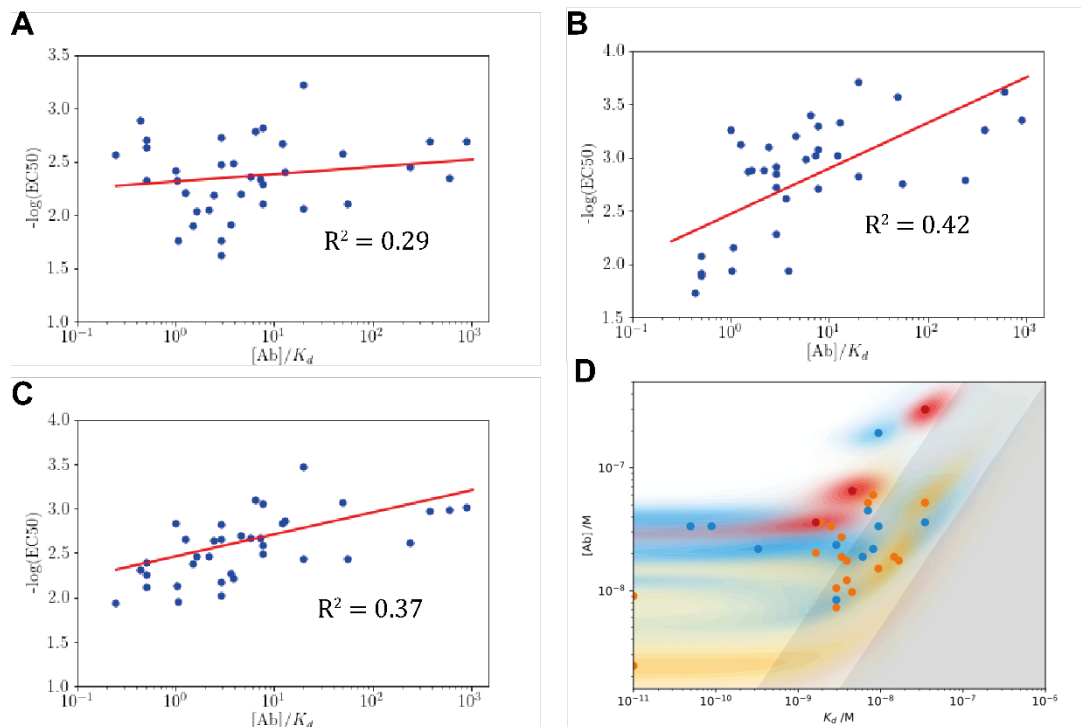


Figure S1: Correlation of $[\text{Ab}]/K_d$ determined by MAAP with ELISA data from¹ for the same individuals. (A) pEC50 spike, (B) pEC50 RBD and (C) pEC50 average of RBD and spike. This shows that there is a clear trend in correlation, although this trend is not perfectly linear. (D) Probability distributions of dissociation constants, K_d , and antibody concentrations in Figure 2B, with distinction between healthy volunteers (blue), PCR confirmed convalescent (orange) and severe (red) patients. Points correspond to the maximum probability values in the two-dimensional probability distribution, and shaded regions to the probability density. We do not observe significant difference in either K_d or concentration between different symptom severities.

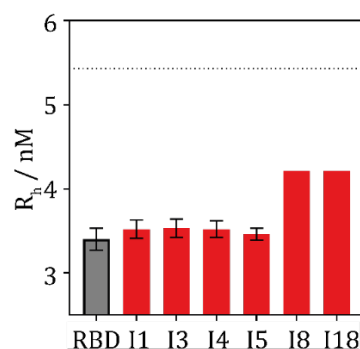


Figure S2: Samples that didn't show binding against the RBD domain using microfluidics. Comparison of the hydrodynamic radius, R_h , of these samples at 40% plasma concentration with 10 nM [RBD] compared to the expected minimum size increase (dotted line) observed for the other individuals in the same cohort under the same conditions and to the hydrodynamic radius of pure RBD. This shows that samples of individuals I1, I3, I4, I5, I8 and I18 do not have any detectable binding to RBD using our microfluidics technology. Hence the quantification of the K_d and antibody concentration is impossible for these samples.

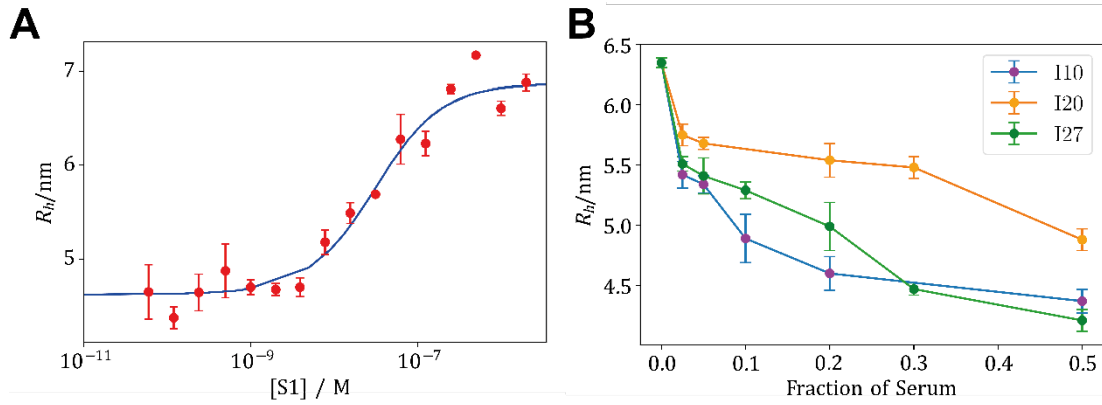


Figure S3: ACE2 competition, **(A)** Binding curve of ACE2 against S1 protein, showing a $K_d = 27.3$ nM. Error bars are the standard deviation from triplicate measurements. **(B)** Dilution series, showing concentration dependent decrease of hydrodynamic radii in three COVID-19 infected individuals in the competition assay outlined in Figure 3.

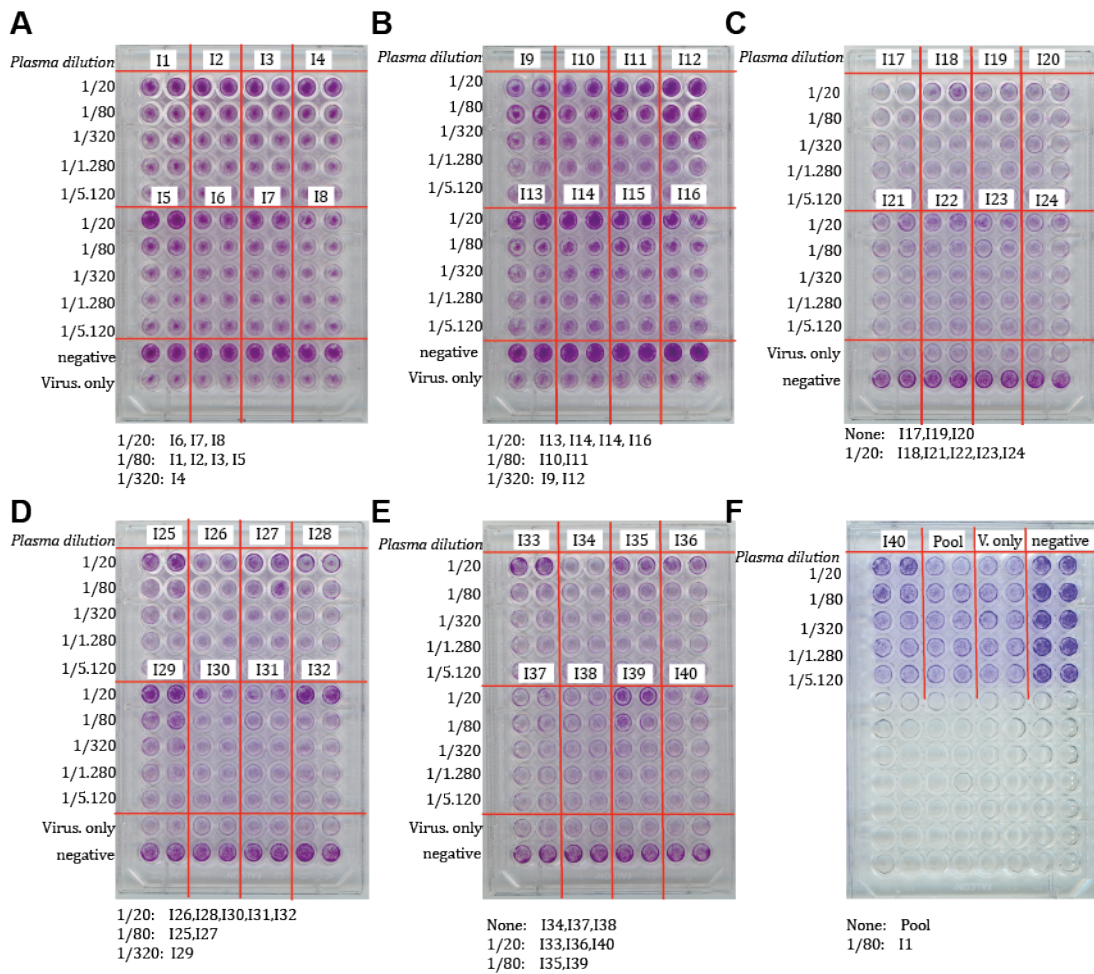


Figure S4: Cell-plaque neutralisation assay. Overview over all plates with the respective interpretation below the images.

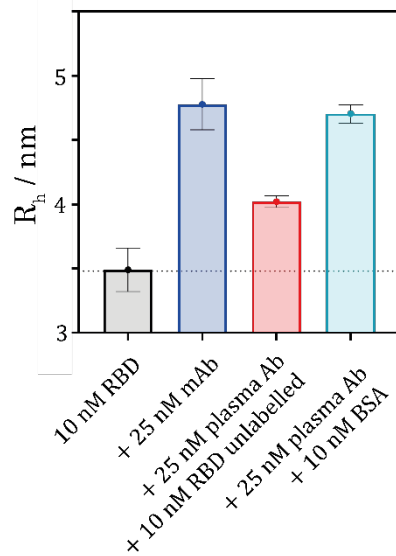


Figure S5: Competition assay. 10 nM labelled RBD SARS-CoV-2 was incubated in 25 nM antibodies of plasma samples from seropositive individuals. When incubated in additional presence of 10 nM unlabelled RBD SARS-CoV-2, the radius decreased significantly, whilst the radius remained the same upon addition of BSA. Error bars are standard deviation from triplicate measurement.

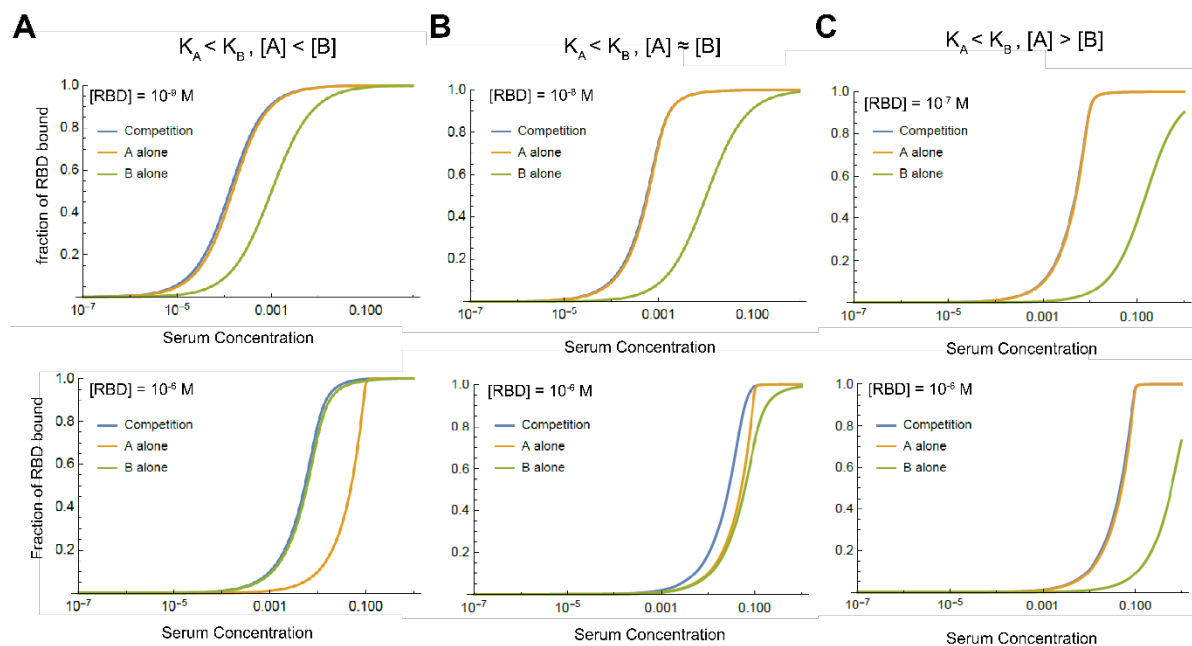


Figure S6: Simulation of competition of two antibodies with $K_A = 10^{-9}$ M and $K_B = 10^{-7}$ M. **(A)** For the case that $[A] < [B]$, there are two subregimes: if the RBD concentration is around or lower than K_A , the combined behaviour resembles that of the stronger binding species, if it is present around or above the higher equilibrium constant, K_B , then it resembles the weaker binding species. In between, the behaviour is intermediate. **(B)** For the situation that $[A] \approx [B]$, the combined response is dominated by the tighter binder in both high and low RBD concentration. **(C)** For $[A] > [B]$, the signal measured is determined by the tightly binding antibody.

Table S1. Demographic characterisation of the individuals used in our study.

Cohort	Total number	Number male	Number female	Number undefined	Median age (IQR) - years
Convalescent individuals	19	19	0	0	27 (22-49)
Healthy blood donors	20	8	10	2	31 (24-45)
Hospital patients	3	2	1	0	67 (65-74)

Table S2: Comparison of results on ACE2 competition and Cell-Plaque Neutralisation assay.

ACE2 \ Virus Neut.	positive	negative	total
positive	30	1	31
negative	2	4	6
total	32	5	

- 1 Emmenegger, M. *et al.* Early plateau of SARS-CoV-2 seroprevalence identified by tripartite immunoassay in a large population. *medRxiv*, 2020.2005.2031.20118554, doi:10.1101/2020.05.31.20118554 (2020).